

Entanglement and coherence in bi-squeezed tripartite Gaussian states

David Edward Bruschi,¹ Carlos Sabín,² and Gheorghe Sorin Paraoanu³

¹*York Centre for Quantum Technologies, Department of Physics,
University of York, Heslington, YO10 5DD York, UK*

²*Instituto de Física Fundamental (CSIC), Serrano 113-bis, 28006 Madrid, Spain*

³*Low Temperature Laboratory and Centre for Quantum Engineering,
Department of Applied Physics, Aalto University School of Science, FI-00076 Aalto, Finland*

We study the properties of bi-squeezed tripartite Gaussian states that can be produced in the laboratory by double parametric pumping of the electromagnetic field modes confined in a resonator. We focus on the quantification of the quantum correlations across of all partitions, as well as on the genuine multipartite entanglement, obtaining analytical expressions for most of the quantities of interest. We find that the state contains genuine tripartite entanglement as well as bipartite entanglement among the modes that are directly squeezed. We also consider the effect of homodyne detection of the photons in the common-mode (coupled by both pumps), and analyse the final reduced state of the remaining two modes. The quantum coherence between the modes that are not squeezed can be converted into entanglement by means of a homodyne detection of the remaining mode.

I. INTRODUCTION

The nature of the vacuum in quantum theory is not intuitive. The classical picture of a “void” or “emptiness” does not accurately capture the nature of this particular state and new phenomena can be unveiled when the quantum formalism is systematically employed [1]. One way to better understand the quantum vacuum is to adopt the following view. A quantum state is the vacuum state only with respect to a particular Hamiltonian. In this language, the vacuum state can be defined as the lowest energy eigenstate of a particular Hamiltonian, which does not imply that it will be the lowest energy eigenstate of another Hamiltonian, which might arise from a particular transformation of the original one. One can picture the “vacuum” as a state with some latent structure (*e.g.*, see [2]), which can manifest, for example, through the conversion of quantum fluctuations into real excitations when well-chosen operations are performed on the state (*i.e.*, sudden quench, parametric driving, *etc.*). This phenomenon is generally known as dynamical Casimir Effect [3] and is typically depicted by a mirror moving in vacuum at relativistic speeds [4]. This can be achieved in the laboratory by using superconducting circuit devices [5, 6]. In these scenarios, abrupt modifications of the boundary conditions [5] or of the speed of light in a meta-material [6] by means of an external pump result in field excitations that can be amplified and detected. These processes give rise to two-mode squeezed microwaves which display entanglement [6] and other forms of quantum correlation [7–9], triggering the question of their employability as resources for quantum technologies [10, 11].

Recently, it has been reported that a new class of three-mode states can be generated in the laboratory by double-pumping a superconducting resonator [12]. This can be regarded as a “double dynamical Casimir effect”, since now the mirror moves under the action of two pumps with different frequencies - or, in other words, the motion of the mirror is a harmonic oscillation with the av-

erage frequency of the pumps modulated due to beating at half-difference frequency. One starts by considering three modes a, b and c . The two pumps generate two-mode squeezing among modes $a-b$ and $b-c$ respectively. However we show that the resulting tripartite state does not only contain the standard correlations due to parametric two-mode squeezing but it also displays correlations among the modes a and c , even if these modes are not directly connected by the pumps. In this work we provide a systematic analysis of the quantum correlation properties of the aforementioned class of tripartite Gaussian states. We find that there exists genuine tripartite entanglement above a threshold value of the initial squeezing parameter as well as $a-b$ and $b-c$ entanglement, but no $a-c$ entanglement. Surprisingly, we find that the quantum coherence between modes a and c becomes entanglement after the homodyne detection of mode b .

This paper is organised as follows. In Section II we introduce the essential tools from quantum optics with continuous variables and the covariance matrix mathematical formalism. In Section III we study the genuine multipartite entanglement generated, as well as the bipartite entanglement generated across all reduced states. In Section IV we will analyse the state of two chosen modes after the application of homodyne detection of the third one. In Section V we study a few applications of these techniques to realistic scenarios, such as experiments at low temperatures or modes with very close frequencies.

We use the following conventions: bold symbols stand for matrices and plain font with under scripts denote elements of vectors and matrices. In this work Tp stands for transposition, in order to avoid confusion with temperature, denoted by T , and time, denoted by t .

II. CONTINUOUS VARIABLES AND GAUSSIAN STATES

In this work we restrict our attention to Gaussian states of bosonic fields only. Gaussian states are a class of quantum states that enjoy remarkable properties, in particular when the transformations involved are linear unitary transformations, i.e. they are quadratic in the creation and annihilation operators [13]. In this case, the Gaussian character of the state is preserved and one can employ techniques from the Covariance Matrix formalism [13]. Gaussian states of bosonic fields naturally occur in many experiments and, when applicable, offer a convenient description of the state of the electromagnetic field in the optical or microwave range [13].

In this section we briefly introduce the Covariance Matrix formalism, which is a powerful tool that can be used when considering unitary linear transformations between Gaussian states of bosonic fields.

A. Symplectic matrices

We start by considering N bosonic modes (e.g., harmonic oscillators) with annihilation and creation operators $\{a_n, a_n^\dagger\}$. These operators satisfy the standard canonical commutation relations $[a_n, a_{n'}^\dagger] = \delta_{nn'}$, while all other commutators vanish. It is convenient to collect all the operators and introduce the vector $\mathbb{X} := (a_1, a_2, \dots, a_N; a_1^\dagger, a_2^\dagger, \dots, a_N^\dagger)^{\text{Tp}}$, where Tp stands for transpose. For example, we have that $\mathbb{X}_2 = a_2$ or $\mathbb{X}_{2N-1} = a_{N-1}^\dagger$ with this choice of operator ordering. We notice in passing that the techniques developed below can be extended in a straightforward fashion to an infinite number of bosonic operators. This situation occurs, for example, in quantum field theory in flat and curved spacetime [4].

The canonical commutation relations can now be written as $[\mathbb{X}_n, \mathbb{X}_m^\dagger] = i\Omega_{nm}$, where Ω_{nm} are the elements of the $2N \times 2N$ matrix Ω , known as symplectic form, which has the following explicit form

$$i\Omega = \begin{pmatrix} \mathbb{1} & 0 \\ 0 & -\mathbb{1} \end{pmatrix}. \quad (1)$$

Here $\mathbb{1}$ are the $N \times N$ identity matrices.

Any unitary transformation $U = \exp[-iH]$, with Hermitian generator H that is quadratic in the creation and annihilation operators (or, equivalently, in the quadrature operators), induces a *linear transformation* on the (collection of) operators \mathbb{X} through the equation $U^\dagger \mathbb{X} U = \mathbf{S} \mathbb{X}$. The unitary operators in the expression $U^\dagger \mathbb{X} U$ act on each element of the vector \mathbb{X} independently and \mathbf{S} is a symplectic matrix that takes the form $\mathbf{S} = \exp[-F\Omega H]$, where F is a real function that needs to be determined and H is defined through $H = \mathbb{X}^\dagger H \mathbb{X}$.

The matrix \mathbf{S} is called symplectic since it satisfies $\mathbf{S} \Omega \mathbf{S}^\dagger = \Omega$ or, equivalently, $\mathbf{S}^\dagger \Omega \mathbf{S} = \Omega$. Notice that

this implies that $\det(\mathbf{S}) = \pm 1$ and we will focus on transformations with positive determinant, i.e., $\det(\mathbf{S}) = 1$.

A symplectic matrix \mathbf{S} can always be written, with the particular choice of operator ordering in \mathbb{X} , as

$$\mathbf{S} = \begin{pmatrix} \boldsymbol{\alpha} & \boldsymbol{\beta} \\ \boldsymbol{\beta}^* & \boldsymbol{\alpha}^* \end{pmatrix}. \quad (2)$$

The $N \times N$ matrices $\boldsymbol{\alpha}$ and $\boldsymbol{\beta}$, in the case of quantum fields and curved spacetime, collect the well known Bogoliubov coefficients used extensively in literature [4]. These coefficients satisfy the well known Bogoliubov identities [4], which read $\boldsymbol{\alpha} \boldsymbol{\alpha}^\dagger - \boldsymbol{\beta} \boldsymbol{\beta}^\dagger = \mathbb{1}$ and $\boldsymbol{\alpha} \boldsymbol{\beta}^{Tp} - \boldsymbol{\beta} \boldsymbol{\alpha}^{Tp} = 0$ in compact form.

We finally notice that all the machinery introduce here can be introduced *independently* of the initial state of the system.

B. Gaussian states

Unitary evolution and transformations, represented by a unitary operator U , of bosonic systems which are initially in a state ρ_i are of great importance in physics. Unitary evolution leads to a final state ρ_f through the standard Heisenberg equation $\rho_f = U^\dagger \rho_i U$. If the state ρ_i is a Gaussian state, and the unitary U is a linear operator (see above), the Gaussian character is preserved; therefore, employing the specific results of Gaussian state formalism becomes very convenient [13].

In general, a state ρ of N bosonic modes is defined by an infinite amount of degrees of freedom. However, a Gaussian state ρ of bosonic modes is characterised only by a finite amount of degrees of freedom. In particular, it is uniquely defined by the vector d of first moments and the second moments σ_{nm} defined by $d := \langle \mathbb{X} \rangle_\rho$ and $\sigma_{nm} := \langle \{\mathbb{X}_n, \mathbb{X}_m^\dagger\} \rangle_\rho - 2\langle \mathbb{X}_n \rangle_\rho \langle \mathbb{X}_m^\dagger \rangle_\rho$ respectively, see [13]. Here, all expectation values $\langle \mathcal{O} \rangle_\rho$ of an operator \mathcal{O} are defined by $\langle \mathcal{O} \rangle_\rho := \text{Tr}(\mathcal{O}\rho)$ and $\{A, B\} = AB + BA$ is the anticommutator of operators A and B . In this work we ignore the first moments, which can be safely set to zero without loss of generality. We make this choice since we are interested in quantum correlations, which are unaffected by the first moments. Initial vanishing moments remain vanishing under symplectic transformations and the second moments σ_{nm} can be conveniently collected into the Hermitian covariance matrix $\boldsymbol{\sigma}$, see [13]. We notice that a covariance matrix $\boldsymbol{\sigma}$ represents a physical state ρ if it satisfies $\boldsymbol{\sigma} + i\Omega \geq 0$ in the operatorial sense [13]. This amounts to computing the eigenvalues of the matrix $\boldsymbol{\sigma} + i\Omega$ and checking if they are positive.

We can now recast the Heisenberg equation $\rho_f = U^\dagger \rho_i U$ into a relation between covariance matrices. Let the initial state ρ_i be represented by the covariance matrix $\boldsymbol{\sigma}_i$ and the final state ρ_f by the covariance matrix $\boldsymbol{\sigma}_f$. We have already seen that any quadratic unitary U can be represented by a symplectic matrix \mathbf{S} . Then, the Heisenberg equation $\rho_f = U^\dagger \rho_i U$ takes the form

$\sigma_f = S^\dagger \sigma_i S$, which reduces the problem of usually untreatable operator algebra to matrix multiplication of $2N \times 2N$ matrices.

Williamson's theorem [14–16] guarantees that any covariance matrix σ can be put in diagonal form by a symplectic matrix. This means that, given a covariance matrix σ it is always possible to find a symplectic matrix s such that $\sigma = s^\dagger \nu_{\oplus} s$, where the diagonal matrix $\nu_{\oplus} = \text{diag}(\nu_1, \nu_2, \dots, \nu_N; \nu_1, \nu_2, \dots, \nu_N)$ is called the Williamson form of σ and $\nu_m \geq 1$ are called the symplectic eigenvalues of σ . The symplectic eigenvalues $\{\nu_m\}$ are obtained as the eigenvalues of the matrix $i\Omega\sigma$. The purity P of the state σ is given by $P = \prod_m \nu_m \geq 1$, and the state is pure if $P = 1$ (or, equivalently, $\nu_m = 1$ for all m).

A $2N \times 2N$ covariance matrix σ is a Hermitian matrix that can be written in the form

$$\sigma = \begin{pmatrix} \mathbf{U} & \mathbf{V} \\ \mathbf{V}^* & \mathbf{U}^* \end{pmatrix}, \quad (3)$$

where the $N \times N$ matrices \mathbf{U} and \mathbf{V} satisfy $\mathbf{U} = \mathbf{U}^\dagger$ and $\mathbf{V} = \mathbf{V}^{T_p}$.

C. Useful properties of the covariance matrix

In this subsection we provide some useful insight on some properties enjoyed by elements of covariance matrices. We start by introducing the symplectic eigenvalues ν_m . These eigenvalues can be written as $\nu_m = \coth(\frac{\hbar\omega_m}{2k_B T})$, where T is the temperature of the one-mode reduced state. This property is also related to the fact that every single-mode reduced state of a Gaussian state is a thermal state up to local operations [13]. Notice that if a state σ is a thermal state then it coincides with its Williamson form, i.e., $\sigma \equiv \nu_{\oplus}$.

An important operation is the process of “tracing out” a particular subsystem. In this language, this operation just amounts to deleting the rows and columns corresponding to the system one wishes to trace out [13].

As a useful application, we now show how we can employ the covariance matrix to compute interesting quantities. Let $\langle a_m^\dagger a_m \rangle_\rho$ be the number expectation value of mode m . Without loss of generality, let us assume that the first moments vanish, i.e., $\langle \mathbb{X} \rangle = 0$. Then it is easy to show that $\langle a_m^\dagger a_m \rangle_\rho = \frac{1}{2}[\sigma_{mm} - 1]$, which highlights the role of the covariance matrix when computing physically relevant quantities.

D. Entanglement in Gaussian states

The quantitative characterisation of entanglement is a central task in many areas of quantum science. For example, entanglement is at the core of quantum computation [17, 18], quantum cryptography and quantum communication [19]. For two modes in general, and for Gaussian

states in particular, the task has been fully solved and in an unambiguous way and entanglement has been completely characterised [13].

It has been shown that every measure of entanglement for two mode Gaussian states is a function of the *smallest symplectic eigenvalue* of the partial transpose [13]. This establishes the PPT criterion as the paramount criterion for two-mode Gaussian states. One starts from the two mode state σ and obtains the partial transpose $\tilde{\sigma}$ as $\tilde{\sigma} = \mathbf{P} \sigma \mathbf{P}$ where the partial transposition matrix \mathbf{P} takes the form

$$\mathbf{P} = \begin{pmatrix} 1 & 0 & 0 & 0 \\ 0 & 0 & 0 & 1 \\ 0 & 0 & 1 & 0 \\ 0 & 1 & 0 & 0 \end{pmatrix}. \quad (4)$$

One then computes the symplectic eigenvalues $\{\tilde{\nu}_m\}$ of the partial transpose $\tilde{\sigma}$ as $\{\tilde{\nu}_m\} = \text{Spect}(i\Omega\tilde{\sigma})$. These eigenvalues come in two pairs of identical eigenvalues and we denote the smallest one as $\tilde{\nu}_-$. If $\tilde{\nu}_- < 1$ then there is entanglement.

The choice of a particular measure is a matter of convenience or of the problem at hand, since all measures are (decreasing) monotonic functions of $\tilde{\nu}_-$. We can choose the negativity \mathcal{N} defined as

$$\mathcal{N} := \max \left[0, \frac{1 - \tilde{\nu}_-}{2\tilde{\nu}_-} \right], \quad (5)$$

or the logarithmic negativity $E_{\mathcal{N}}$ defined as

$$E_{\mathcal{N}} := \max [0, -\ln(\tilde{\nu}_-)]. \quad (6)$$

We can also choose the entanglement of formation \mathcal{E}_{oF} defined as

$$\mathcal{E}_{\text{oF}} := \max [0, f_+(\tilde{\nu}_-) - f_-(\tilde{\nu}_-)], \quad (7)$$

where we have introduced the functions $f_{\pm}(x) := \frac{(x \pm 1)^2}{4x} \ln \frac{(x \pm 1)^2}{4x}$ for convenience of presentation.

E. An example: Two-mode squeezing

As an example let us look at two mode squeezing. Let $\mathbb{X} := (a, b, a^\dagger, b^\dagger)$. The unitary operator that implements two mode squeezing is $U(r) = \exp[r(a^\dagger b^\dagger - a b)]$ and it is easy to show that in this (simplified) case its symplectic representation is

$$\mathbf{S} = \begin{pmatrix} \cosh r & 0 & 0 & \sinh r \\ 0 & \cosh r & \sinh r & 0 \\ 0 & \sinh r & \cosh r & 0 \\ \sinh r & 0 & 0 & \cosh r \end{pmatrix}. \quad (8)$$

Notice that we have chosen a special case where the transformation is real, for the sake of simplicity and without any loss of generality. We can define the vector

$\tilde{\mathbb{X}} := (\tilde{a}, \tilde{b}, \tilde{a}^\dagger, \tilde{b}^\dagger) = \mathbf{S} \mathbb{X}$ of new operators. The two mode squeezing transformation reduces to its well-known form

$$\begin{aligned}\tilde{a} &= \cosh r a + \sinh r b^\dagger, \\ \tilde{b} &= \cosh r b + \sinh r a^\dagger.\end{aligned}\quad (9)$$

In the usual Fock state formalism, the two-mode squeezed state $|\psi(r)\rangle$ of two modes a and b has the form

$$|\psi(r)\rangle = \sum_{n=0}^{+\infty} \frac{\tanh^n r}{\cosh r} |n, n\rangle_{ab}. \quad (10)$$

In the covariance matrix formalism, we can easily see that the two mode squeezed state (10) takes the form

$$\boldsymbol{\sigma} = \begin{pmatrix} \cosh 2r & 0 & 0 & \sinh 2r \\ 0 & \cosh 2r & \sinh 2r & 0 \\ 0 & \sinh 2r & \cosh 2r & 0 \\ \sinh 2r & 0 & 0 & \cosh 2r \end{pmatrix}. \quad (11)$$

This explicitly shows how Gaussian states in the Fock state formalism reduce to simple matrices in the Gaussian state formalism.

We now proceed and compute the spectrum $\{\tilde{\nu}_m\}$ of the matrix $i\boldsymbol{\Omega} \mathbf{P} \boldsymbol{\sigma} \mathbf{P}$, which is the set of the symplectic eigenvalues of the partial transpose of the state (11). It is easy to show that they are $\{\tilde{\nu}_m\} = (e^{2r}, e^{2r}, e^{-2r}, e^{-2r})$. We see that the smallest symplectic eigenvalue $\tilde{\nu}_-$ has the expression $\tilde{\nu}_- = e^{-2r}$. This implies that the logarithmic negativity E_N reads $E_N = 2r$. Once more, this underlines the power of this formalism.

III. GENERATION OF BI-SQUEEZED TRI-PARTITE GAUSSIAN STATES

We now move to the physical system of interest. The system we consider in this work is composed of three bosonic modes a, b, c with frequencies $\omega_a, \omega_b, \omega_c$ respectively. The three modes are modulated parametrically by two pump fields at the frequencies $\omega_{ab}^{(p)}$ and $\omega_{bc}^{(p)}$. Systems of this type have been realised and measured in the laboratory, for example in a superconducting resonator [12]. The total Hamiltonian H for this type of configuration can be constructed by adding to the harmonic-oscillator Hamiltonian $H_0 = \hbar\omega_a a^\dagger a + \hbar\omega_b b^\dagger b + \hbar\omega_c c^\dagger c$ of the three modes, two parametric perturbations corresponding to each pump [20]. One obtains the total Hamiltonian H of the form

$$H = H_0 + \hbar \left(\chi_{ab}^* e^{i\omega_{ab}^{(p)} t} a b + \chi_{bc}^* e^{i\omega_{bc}^{(p)} t} b c + \text{h.c.} \right). \quad (12)$$

Here χ_{ab} and χ_{bc} have dimensions of frequencies and describe the parametric coupling of the pumping fields into the modes a, b, c , representing the parametric analog of the Rabi frequency of driven two-level systems. This prescription is very general, irrespective to the particular physical system employed or to whether the modulation

is done on the boundary conditions or in the bulk of the material or device (see *e.g.* Supporting Information in [6] and [21]). Consider now the unitary transformation $U_0(t) = \exp[-\frac{i}{\hbar} H_0 t]$. Assuming that the frequencies of the pumps $\omega_{ab}^{(p)}$ and $\omega_{bc}^{(p)}$ are chosen such that the energy conservation conditions $\omega_{ab}^{(p)} = \omega_a + \omega_b$ and $\omega_{bc}^{(p)} = \omega_b + \omega_c$ are satisfied, the Hamiltonian (12) can be transformed into $H_{\text{eff}} = U_0(t)^\dagger H U_0(t) + i\hbar[dU_0^\dagger(t)/dt]U_0(t)$, where we have defined

$$H_{\text{eff}} = \hbar(\chi_{ab}^* a b + \chi_{bc}^* b c + \text{h.c.}). \quad (13)$$

The effective Hamiltonian H_{eff} is now time-independent and describes the evolution of the system in a triple rotating frame (with frequencies $\omega_a, \omega_b, \omega_c$). Suppose now that the system is pumped for a finite time τ , as it was done in the time-domain experiments in previous work [12]. Then, introducing the two mode squeezing operators $G_{ab} := a^\dagger b^\dagger + a b$ and $G_{bc} := b^\dagger c^\dagger + b c$ and the corresponding two-mode squeezing parameters $R_{ab} = -\chi_{ab}^* \tau$ and $R_{bc} = -\chi_{bc}^* \tau$ we get

$$U = e^{i[R_{ab} G_{ab} + R_{bc} G_{bc}]} \quad (14)$$

We emphasize that this structure of the evolution operator is very general. Indeed, it can be recovered also for continuous pumping and for systems with dissipation in the input-output formalism [12].

To investigate systematically the correlations induced by this operator, we collect the creation and annihilation operators of these modes in the vector $\mathbb{X} = (a, b, c, a^\dagger, b^\dagger, c^\dagger)^T p$. We assume that the initial state is a thermal state $\boldsymbol{\sigma}_{th}$ at temperature T , since temperature is always present in any realistic system. The state $\boldsymbol{\sigma}_{th}$ of the system just coincides with its Williamson form, i.e., $\boldsymbol{\sigma}_{th} = \boldsymbol{\nu}_\oplus = \text{diag}(\nu_a, \nu_b, \nu_c, \nu_a, \nu_b, \nu_c)$.

Next, we proceed to construct the final state of interest ρ , represented by the covariance matrix $\boldsymbol{\sigma}$, that we obtain by applying the operator to the thermal state $\boldsymbol{\sigma}_{th}$. For simplicity, we assume that the squeezing parameters R_{ab} and R_{bc} are both real.

It is not possible to compute the state ρ in the Fock state formalism, and it is also extremely difficult to compute the symplectic matrix \mathbf{S} representing the operator (14). In fact, regardless of how simple the combination of operators might look like in (14), the algebra involved requires decoupling all operators into *generators* of the $SL(3, \mathbb{C})$ group as explained more in detail below.

Here we will use a recently-developed technique [22, 23] (see also [24] for an alternative approach) to obtain more convenient representations of the operator (14), based on the Lie algebra structure of the $SL(3, \mathbb{C})$ group [16]. In Appendix A we show that it is possible to re-write the operator (14) as

$$U = e^{i\theta_{ac} B_{ac}} e^{i r_{ab} G_{ab}} e^{i r_{bc} G_{bc}}, \quad (15)$$

where the real squeezing parameters r_{ab}, r_{bc} and phase

θ_{ac} have the *exact* expression

$$\begin{aligned} r_{ab} &= \ln \left(\cos \phi \sinh \rho + \sqrt{1 + \cos^2 \phi \sinh^2 \rho} \right), \\ r_{bc} &= \frac{1}{2} \ln \left(\frac{1 + \sin \phi \tanh \rho}{1 - \sin \phi \tanh \rho} \right), \\ \theta_{ac} &= \arctan \left(\frac{\tan \phi}{\cosh \rho} \right) - \phi, \end{aligned} \quad (16)$$

as functions of the new parameters $\rho := \sqrt{R_{ab}^2 + R_{bc}^2}$ and $\tan \phi := R_{bc}/R_{ab}$. Here $B_{ac} = i [a c^\dagger - c a^\dagger]$ is a beam-splitter transformation. The result is remarkable, because in general it is not possible to obtain simple analytical solutions when trying to factorize an exponential of multiple-mode operators using the well-known Hausdorff-Baker-Campbell approach to decoupling exponentials. We emphasise that the unitary operators (14) and (15) are equivalent, and the final state obtained under their action is also the same. We also note that the factorized representation (15) can be used as well as a heuristic tool in designing novel experiments, since the bi-squeezed Gaussian state obtained by double parametric pumping can then be created alternatively by pumping first one pair of modes, then another pair, and finally performing a beam-splitter transformation. For example, in quantum optics it might be convenient to even use two different crystals for realizing the two squeezing operations.

In order to obtain the correlation matrix, our task is now to start by applying a beam splitting $\mathbf{S}_{ac}(\theta_{ac})$ on modes a and c which, in symplectic geometry, has the form

$$\mathbf{S}_{ac}(\theta_{ac}) = \begin{pmatrix} \cos \theta_{ac} & 0 & \sin \theta_{ac} & 0 & 0 & 0 \\ 0 & 1 & 0 & 0 & 0 & 0 \\ -\sin \theta_{ac} & 0 & \cos \theta_{ac} & 0 & 0 & 0 \\ 0 & 0 & 0 & \cos \theta_{ac} & 0 & \sin \theta_{ac} \\ 0 & 0 & 0 & 0 & 1 & 0 \\ 0 & 0 & 0 & -\sin \theta_{ac} & 0 & \cos \theta_{ac} \end{pmatrix}. \quad (17)$$

Notice that this would be a trivial operation if the state was the vacuum however, the initial state is thermal and the beamsplitter can have a non-trivial effect.

We proceed by applying a two mode squeezing $\mathbf{S}_{ab}(r_{ab})$ on modes a and b and a two mode squeezing $\mathbf{S}_{bc}(r_{bc})$ on modes b and c . These have the form

$$\mathbf{S}_{ab}(r_{ab}) = \begin{pmatrix} \text{ch}_{ab} & 0 & 0 & 0 & \text{sh}_{ab} & 0 \\ 0 & \text{ch}_{ab} & 0 & \text{sh}_{ab} & 0 & 0 \\ 0 & 0 & 1 & 0 & 0 & 0 \\ 0 & \text{sh}_{ab} & 0 & \text{ch}_{ab} & 0 & 0 \\ \text{sh}_{ab} & 0 & 0 & 0 & \text{ch}_{ab} & 0 \\ 0 & 0 & 0 & 0 & 0 & 1 \end{pmatrix}. \quad (18)$$

and

$$\mathbf{S}_{bc}(r_{bc}) = \begin{pmatrix} 1 & 0 & 0 & 0 & 0 & 0 \\ 0 & \text{ch}_{bc} & 0 & 0 & 0 & \text{sh}_{bc} \\ 0 & 0 & \text{ch}_{bc} & 0 & \text{sh}_{bc} & 0 \\ 0 & 0 & 0 & 1 & 0 & 0 \\ 0 & 0 & \text{sh}_{bc} & 0 & \text{ch}_{bc} & 0 \\ 0 & \text{sh}_{bc} & 0 & 0 & 0 & \text{ch}_{bc} \end{pmatrix}, \quad (19)$$

where we have introduced $\text{ch}_{ab} := \cosh r_{ab}$, $\text{sh}_{ab} := \sinh r_{ab}$, $\text{th}_{ab} := \tanh r_{ab}$ and $\text{ch}_{bc} := \cosh r_{bc}$, $\text{sh}_{bc} := \sinh r_{bc}$, $\text{th}_{bc} := \tanh r_{bc}$ for compactness and simplicity of presentation.

The final state, when acting on the thermal state $\boldsymbol{\sigma}_{th} = \text{diag}(\nu_a, \nu_b, \nu_c, \nu_a, \nu_b, \nu_c)$ as well as all the reduced states, can be obtained analytically, see Appendix B for the full expressions of each matrix element. Here we report only the structure of these states, which is essential for the ensuing calculations. The (three-mode) state $\boldsymbol{\sigma}$ reads

$$\boldsymbol{\sigma} = \begin{pmatrix} \alpha & 0 & \delta & 0 & \epsilon & 0 \\ 0 & \beta & 0 & \epsilon & 0 & \zeta \\ \delta & 0 & \gamma & 0 & \zeta & 0 \\ 0 & \epsilon & 0 & \alpha & 0 & \delta \\ \epsilon & 0 & \zeta & 0 & \beta & 0 \\ 0 & \zeta & 0 & \delta & 0 & \gamma \end{pmatrix}. \quad (20)$$

The final two-mode $\boldsymbol{\sigma}^{(ab)}, \boldsymbol{\sigma}^{(bc)}, \boldsymbol{\sigma}^{(ac)}$ and single-mode states $\boldsymbol{\sigma}^{(a)}, \boldsymbol{\sigma}^{(b)}, \boldsymbol{\sigma}^{(c)}$ read

$$\begin{aligned} \boldsymbol{\sigma}^{(ab)} &= \begin{pmatrix} \alpha & 0 & 0 & \epsilon \\ 0 & \beta & \epsilon & 0 \\ 0 & \epsilon & \alpha & 0 \\ \epsilon & 0 & 0 & \beta \end{pmatrix} & \boldsymbol{\sigma}^{(a)} &= \begin{pmatrix} \alpha & 0 \\ 0 & \alpha \end{pmatrix}, \\ \boldsymbol{\sigma}^{(bc)} &= \begin{pmatrix} \beta & 0 & 0 & \zeta \\ 0 & \gamma & \zeta & 0 \\ 0 & \zeta & \beta & 0 \\ \zeta & 0 & 0 & \gamma \end{pmatrix} & \boldsymbol{\sigma}^{(b)} &= \begin{pmatrix} \beta & 0 \\ 0 & \beta \end{pmatrix}, \\ \boldsymbol{\sigma}^{(ac)} &= \begin{pmatrix} \alpha & \delta & 0 & 0 \\ \delta & \gamma & 0 & 0 \\ 0 & 0 & \alpha & \delta \\ 0 & 0 & \delta & \gamma \end{pmatrix} & \boldsymbol{\sigma}^{(c)} &= \begin{pmatrix} \gamma & 0 \\ 0 & \gamma \end{pmatrix}. \end{aligned} \quad (21)$$

The reduced two-modes and single-mode covariance matrices were obtained using the *trace-out* prescription from Section II C, namely eliminating one, and respectively two, modes from the three-mode matrix (20).

A. Characterising the final state: number expectation value

We can now turn to computing the final number expectation value for all three modes. We have

$$\begin{aligned} \langle a^\dagger a \rangle &= \frac{1}{2} [\alpha - 1], \\ \langle b^\dagger b \rangle &= \frac{1}{2} [\beta - 1], \\ \langle c^\dagger c \rangle &= \frac{1}{2} [\gamma - 1]. \end{aligned} \quad (22)$$

B. Characterising the final state: purity of all reduced states

We wish to understand the correlation structure of the whole state. A rough understanding can be already given by computing the purity of all the reduced states.

Let us start by the purity $P_{th} = \nu_a^2 \nu_b^2 \nu_c^2$ of the initial global tri-partite thermal state, which remains unchanged under our unitary transformations. We then list the initial purities of the thermal state $P_{th}^{ab}, P_{th}^{bc}, P_{th}^{ac}, P_{th}^a, P_{th}^b, P_{th}^c$ which read

$$\begin{aligned} P_{th}^{(ab)} &= \nu_a^2 \nu_b^2 & P_{th}^{(a)} &= \nu_a^2, \\ P_{th}^{(bc)} &= \nu_b^2 \nu_c^2 & P_{th}^{(b)} &= \nu_b^2, \\ P_{th}^{(ac)} &= \nu_a^2 \nu_c^2 & P_{th}^{(c)} &= \nu_c^2. \end{aligned} \quad (23)$$

We now find that the purities of all reduced states of our given state are

$$\begin{aligned} P^{(ab)} &= (\alpha \beta - \epsilon^2)^2 & P^{(a)} &= \alpha^2, \\ P^{(bc)} &= (\beta \gamma - \zeta^2)^2 & P^{(b)} &= \beta^2, \\ P^{(ac)} &= (\alpha \gamma - \delta^2)^2 & P^{(c)} &= \gamma^2. \end{aligned} \quad (24)$$

We see that local purities have changed from the values in (23) to the ones in (24), therefore we expect some correlations between the different modes. We will proceed to study this in the next section.

C. Characterising the final state: entanglement

Here we look at the nature of (quantum) correlations in the tripartite state of interest in this work. We will study the global (genuine) correlations as well as the bipartite correlations across all bipartite reduced states.

1. Tripartite entanglement

A suitable measure of the tripartite entanglement can be obtained through a suitable average of the entanglement of all the bipartitions of the system. For instance, we can consider the tripartite negativity $\mathcal{N}^{(abc)}$ defined by

$$\mathcal{N}^{(abc)} = (\mathcal{N}^{(a-bc)} \mathcal{N}^{(b-ac)} \mathcal{N}^{(c-ab)})^{\frac{1}{3}}, \quad (25)$$

where $\mathcal{N}^{(i-jk)}$ is the negativity of the $i-jk$ bipartition as provided by the partial transposition with respect to the mode i . In Fig. 1 we plot all the $\mathcal{N}^{(i-jk)}$ and the resulting $\mathcal{N}^{(abc)}$.

We notice that there is need for a certain amount of squeezing before genuine multipartite entanglement can be created.

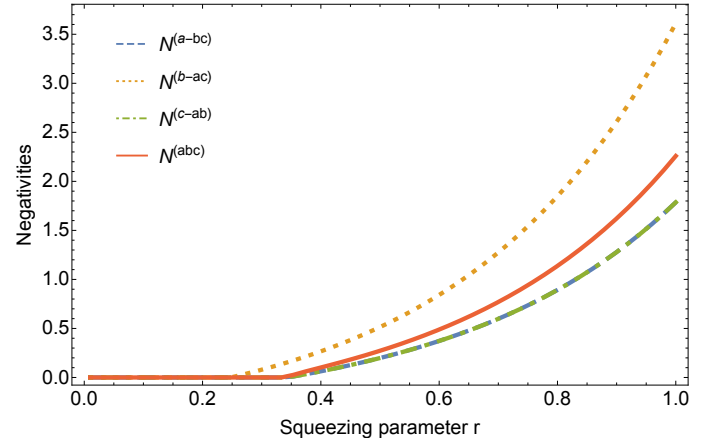


FIG. 1. Tripartite negativity $\mathcal{N}^{(abc)}$, $\mathcal{N}^{(a-bc)}$, $\mathcal{N}^{(b-ac)}$ and $\mathcal{N}^{(c-ab)}$ vs. squeezing parameter $r = R_{ab} = R_{bc}$ for $\omega_a = 2\pi \times 4.99$ GHz, $\omega_b = 2\pi \times 5$ GHz, $\omega_c = 2\pi \times 5.01$ GHz and $T = 15$ mK.

2. Bipartite entanglement in the “ab” and “bc” subsystems

As previously discussed, we now need to compute the smallest symplectic eigenvalue $\tilde{\nu}_-$ for each reduced state. This eigenvalue will provide us with a quantification of entanglement.

We start by the reduced state $\sigma^{(ab)}$ of modes a and b . We can compute the smallest symplectic eigenvalue $\tilde{\nu}_-^{(ab)}$ of the partial transpose and we find

$$\tilde{\nu}_-^{(ab)} = \frac{1}{2} \left[\alpha + \beta - \sqrt{(\alpha - \beta)^2 + 4\epsilon^2} \right]. \quad (26)$$

Similarly, for the reduced state $\sigma^{(bc)}$ of modes b and c we can compute the smallest symplectic eigenvalue $\tilde{\nu}_-^{(bc)}$ of the partial transpose,

$$\tilde{\nu}_-^{(bc)} = \frac{1}{2} \left[\beta + \gamma - \sqrt{(\beta - \gamma)^2 + 4\zeta^2} \right]. \quad (27)$$

These eigenvalue can now be used, together with equation (5) and (7), to compute the negativities $\mathcal{N}^{(ab)}$, $\mathcal{N}^{(bc)}$ as well as the entanglement of formation $\mathcal{E}_{oF}^{(ab)}$, $\mathcal{E}_{oF}^{(bc)}$ in the reduced states $\sigma^{(ab)}$ respectively $\sigma^{(bc)}$.

3. Bipartite entanglement: the “ac” subsystem

We finish with the reduced state $\sigma^{(ac)}$ of modes a and c . We can compute the smallest symplectic eigenvalue $\tilde{\nu}_-^{(ac)}$ of the partial transpose and we find

$$\tilde{\nu}_-^{(ac)} = \frac{1}{2} \left[\sqrt{(\alpha + \gamma)^2 - 4\delta^2} - |\alpha - \gamma| \right]. \quad (28)$$

It is easy to show that $\tilde{\nu}_-^{(ac)} \geq 2|\alpha\gamma - \delta^2|$

This, in turn can be written as $\tilde{\nu}_-^{(ac)} \geq 2\sqrt{P^{(ac)}}$, where $P^{(ac)}$ is the purity of the final reduced state. Since the

purity P of *any* state, in this language, satisfies $P \geq 1$ we conclude that

$$\tilde{\nu}_-^{(ac)} \geq 2, \quad (29)$$

which implies that there can never be any entanglement between the modes a and c , as expected.

D. Characterising the final state: first-order coherence

We conclude this section by noting some peculiar aspects of the “ac” subsystem. We proceed to show that, although the modes a and c have not been directly squeezed and therefore there is no entanglement between them, we still witness the appearance of nontrivial quantum correlations. We will call $\langle a^\dagger c \rangle_\rho$ (first-order) coherence correlation (often denoted by $G_{ac}^{(1)} = \langle a^\dagger c \rangle_\rho$ in optics [20]), and we will quantify it through the term $\langle a^\dagger c \rangle_\rho$. This term can be obtained in a simple way as $\langle a^\dagger c \rangle_\rho = \frac{1}{2} \sigma_{31}$. We find

$$\langle a^\dagger c \rangle_\rho = \frac{\delta}{2}. \quad (30)$$

The mechanism by which these correlations are established reminds the standard which-way information concepts from interferometry. In standard interferometry (or each time we deal with a linear superposition of states) the absence of information about the path that the photon takes (or, equivalently, the information about which specific wave-function within the superposition that constitutes the total wave-function of the particle is “actualized”) results in the formation of an interference pattern. In this case, given a boson occupying mode b , we cannot know from which downconversion process (corresponding to either pump ω_{ab} or ω_{bc}) it originates. We can collect the photons in modes a and c , propagate them in such a way that they acquire a phase difference, and then let them interfere at a screen or detector. We will witness the formation of an interference pattern only if the quantity (30) is non-zero. Therefore, we will refer to $\langle a^\dagger c \rangle_\rho$ as the coherence-correlation between modes a and c . This quantity can be normalized by the power in each mode, and in this case we recover the standard definition of first-order amplitude correlation function from quantum optics applied to modes a, c ,

$$g_{ac}^{(1)} = \frac{\langle a^\dagger c \rangle_\rho}{\sqrt{\langle a^\dagger a \rangle_\rho \langle c^\dagger c \rangle_\rho}}, \quad (31)$$

and using $\langle a^\dagger a \rangle_\rho = (\alpha - 1)/2$ and $\langle c^\dagger c \rangle_\rho = (\gamma - 1)/2$ as determined from (20) we get

$$g_{ac}^{(1)} = \frac{\delta}{\sqrt{(\alpha - 1)(\gamma - 1)}}. \quad (32)$$

Finally, we highlight a connection with many-body physics, where one often finds useful to employ the so-called single-particle density matrix $\rho^{(1)}_{ac}$, see [25, 26].

For our modes a and c , the single-particle density matrix $\rho^{(1)}_{ac}$ is defined as

$$\rho^{(1)}_{ac} = \begin{pmatrix} \langle a^\dagger a \rangle_\rho & \langle a^\dagger c \rangle_\rho \\ \langle c^\dagger a \rangle_\rho & \langle c^\dagger c \rangle_\rho \end{pmatrix} = \frac{1}{2} \begin{pmatrix} \alpha - 1 & \delta \\ \delta & \gamma - 1 \end{pmatrix}. \quad (33)$$

The single-particle density matrix is an essential tool in the study of phase localization [27, 28] and fragmentation of Bose-Einstein condensates [29, 30] - where the vanishing of the off-diagonal element is used as a criterion for fragmentation (the single coherent wavefunction or order parameter associated with condensation breaks into a Fock state). Note that this structure appears already in the matrix $\sigma^{(ac)}$ from (21), but in this form one sees clearly that $\langle a^\dagger c \rangle_\rho$ is the off-diagonal element, thus characterizing the coherence between the modes.

E. Bipartite entanglement and coherence as a function of squeezing

We now proceed to plot the entanglement computed in the previous subsections, as well as the quantum coherence $\langle a^\dagger c \rangle_\rho$. For the entanglement we choose the negativity $\mathcal{N}^{(ij)}$ between modes i and j , where $i, j \in \{a, b, c\}$ as the figure of merit.

In Fig. (2) we see that while $\mathcal{N}^{(bc)} = \mathcal{N}^{(ab)}$ is different from 0 and grows with the initial squeezing, the negativity $\mathcal{N}^{(ac)}$ is 0 for any value of the initial squeezing - as expected. However, we see that a nonzero degree of quantum coherence between a and c exists for any value of the squeezing, as quantified by $\langle a^\dagger c \rangle$. This underlines the fundamental difference between the two-mode correlations produced by a single pump and those produced between the extremal modes in the double dynamical Casimir effect (which have coherence but no entanglement).

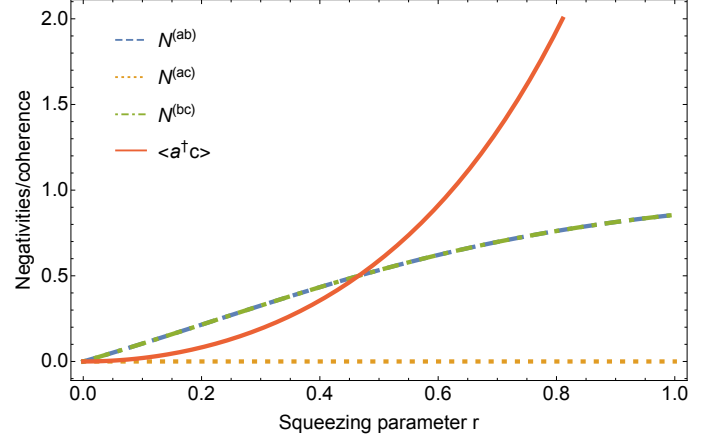


FIG. 2. Bipartite negativities of the reduced states $\mathcal{N}^{(ac)}$, $\mathcal{N}^{(ab)}$, $\mathcal{N}^{(bc)}$ and coherence $\langle a^\dagger c \rangle$ of the a-c reduced state vs. squeezing parameter $r = R_{ab} = R_{bc}$ for $\omega_a = 2\pi \times 4.99$ GHz, $\omega_b = 2\pi \times$ GHz, $\omega_c = 2\pi \times 5.01$ GHz and $T = 15$ mK.

We conclude by noting that, although in the final state the entanglement between modes a and c is vanishingly small, by measuring the mode b in a homodyne scheme one can induce a finite degree of entanglement between modes a and c . This will be demonstrated in the next section.

IV. STATES AFTER HOMODYNE DETECTION

In this section we will compute the resulting state of modes a and c after a *perfect* homodyne detection of mode b . In particular, we will analyse the coherence and entanglement of the resulting state. In order to reach this goal, we will employ the formalism of homodyne detection developed in Ref. 31. The technical computations can be found in Appendix C and we omit them here because they add little to the understanding of the correlations between modes a and c after homodyne detection, which is our main goal.

After lengthy algebra, one has the final state $\sigma_{out|q}^{(ac)}$ of modes a and c after homodyne detection of the quadrature q of mode b , which reads

$$\sigma_{out|q}^{(ac)} = \begin{pmatrix} \alpha - \frac{\epsilon^2}{2\beta} & \delta - \frac{\epsilon\zeta}{2\beta} & -\frac{\epsilon^2}{2\beta} & -\frac{\epsilon\zeta}{2\beta} \\ \delta - \frac{\epsilon\zeta}{2\beta} & \gamma - \frac{\zeta^2}{2\beta} & -\frac{\epsilon\zeta}{2\beta} & -\frac{\zeta^2}{2\beta} \\ -\frac{\epsilon^2}{2\beta} & -\frac{\zeta^2}{2\beta} & \alpha - \frac{\epsilon^2}{2\beta} & \delta - \frac{\epsilon\zeta}{2\beta} \\ -\frac{\epsilon\zeta}{2\beta} & -\frac{\zeta^2}{2\beta} & \delta - \frac{\epsilon\zeta}{2\beta} & \gamma - \frac{\zeta^2}{2\beta} \end{pmatrix}. \quad (34)$$

A simple inspection of the state (34) after homodyne detection underlines the differences with the reduced state $\sigma^{(ac)}$. We see that the coherence δ of the latter is now decreased. In particular, we expect entanglement to be present in the new state (34) since there is a presence of elements in the upper-right part of the state. To prove analytically that there is entanglement requires lengthy formulas, but we will see later that in the case of frequencies that are very close to each other, analytical insight can be gained. The smallest symplectic eigenvalue $\tilde{\nu}_{-}^{out|q}$ of the partial transpose of the state (34) can be computed and has a lengthy expression, which we reproduce in appendix D.

The computation of the negativity of the state (34) after homodyne detection is straightforward and follows step-by-step what has been done above.

In Figure 3 we plot the negativity \mathcal{N} and the coherence $\langle a^\dagger c \rangle$ as a function of the squeezing parameter $r = R_{ab} = R_{bc}$ for realistic values of the frequencies and the temperature. The result is that after the measurement the entanglement becomes nonzero and that the coherence has been reduced after homodyne detection. In other words the state has become more squeezed in the two modes but has lost the coherence term - an extreme situation is the standard two-mode squeezed state, for which the coherence element of the correlation matrix is zero. As mentioned above, more quantitative statements will be made later.

We note that an analog of this effect has been studied with discrete variables: in a tripartite system consisting two superconducting qubits coupled to a resonator with only one quanta of excitation present, a null measurement on the number of particles in the resonator results in the creation of entanglement between the qubits [32, 33], a technique that can be thought of as a particular form of dissipation engineering [34].

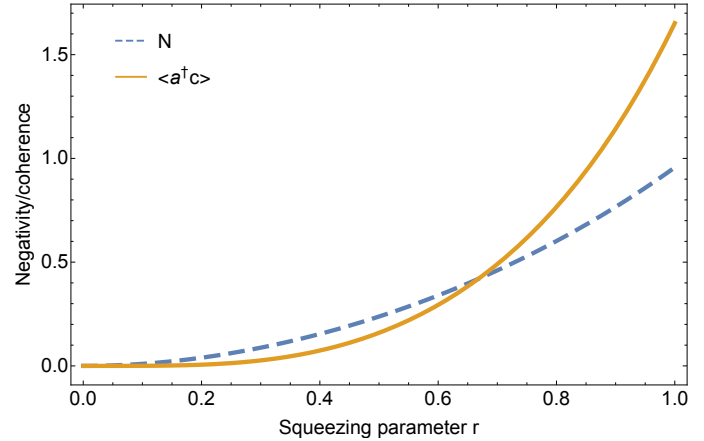


FIG. 3. Negativity and coherence $\langle a^\dagger c \rangle$ vs. squeezing parameter $r = R_{ab} = R_{bc}$ of the state $\sigma_{out|q}^{(ac)}$ for $\omega_a = 2\pi \times 4.99$ GHz, $\omega_b = 2\pi \times 5$ GHz, $\omega_c = 2\pi \times 5.01$ GHz and $T = 15$ mK.

Finally, in Figure 4 we compare the above coherence $\langle a^\dagger c \rangle$ with the other coherences and diagonal elements of the state $\sigma_{out|q}^{(ac)}$.

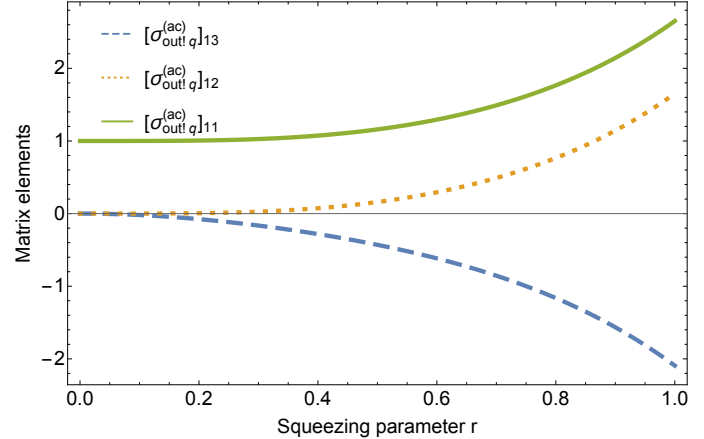


FIG. 4. Elements of the state $\sigma_{out|q}^{(ac)}$ vs. squeezing parameter. Same parameters as in the other figures. $[\sigma_{out|q}^{(ac)}]_{11} = [\sigma_{out|q}^{(ac)}]_{22}$, $[\sigma_{out|q}^{(ac)}]_{13} = [\sigma_{out|q}^{(ac)}]_{14} = [\sigma_{out|q}^{(ac)}]_{24}$, $[\sigma_{out|q}^{(ac)}]_{12}$.

Finally, we argue that testing the prediction of entanglement generation between the modes a and c via homodyne detection in mode b can be done by measuring simultaneously the quadratures of all three modes, then performing post-selection by retaining the data in a and

c that correspond to a certain value of q (or p). Thus, an additional analysis channel needs to be added to the setups used to measure two-frequency correlations in the experiments on the dynamical Casimir effect.

V. APPLICATIONS TO REALISTIC SETUPS

The results presented above can be readily applied to existing experimental setups. We start by noting that we have already analysed the most general scenario possible, i.e., the scenario with initial mixedness due to finite (and not-negligible) temperature and arbitrary frequencies of the modes. This scenario does not allow for further analytical control than the one provided in this work and therefore we have provided numerical results in the figures above.

Entanglement generation depends sensitively on the initial temperature. The other relevant parameter for the experiment is the frequency difference between the modes. In order to discuss scenarios where the relative magnitude of temperature and frequency “compete”, we find it convenient for the discussion below to introduce dimensionless frequencies Ω_m as

$$\Omega_m := \frac{\hbar \omega_m}{k_B T}, \quad (35)$$

where $m = a, b, c$.

This allows us to rewrite the symplectic eigenvalues ν_m as $\nu_m = \coth(\frac{\Omega_m}{2})$, with $m = a, b, c$. Given this redefinition, we can simplify the notations easily and define the reference dimensionless frequency $\Omega := \Omega_b$ and introduce the shift in dimensionless frequencies $\delta\Omega$ through $\Omega - \delta\Omega = \Omega_a$ and $\Omega + \delta\Omega = \Omega_c$. Note that $\delta\Omega/\Omega \leq 1$.

Let us look at some examples. In superconducting circuits, typical values for frequencies are $\omega = 5\text{GHz}$ and $\delta\omega = 10\text{MHz}$ at $T = 15\text{mK}$, while for optical systems we have typically $\omega = 5.64 \times 10^5\text{GHz}$ (532 nm) and $\delta\omega = 0.95\text{GHz}$ at a temperature $T = 300\text{K}$. These numbers translate in $\Omega = 15$ and $\delta\Omega = 0.03$ for superconducting circuits, while $\Omega = 84.6$ and $\delta\Omega = 1.4 \times 10^{-4}$ for optical systems.

The temperatures that one can find in superconducting circuits are ideally of the order of $T = 15\text{mK}$, but higher temperatures are relevant due to imperfect thermalization and nonequilibrium heating effects. The results that we obtain below can be applied to superconducting circuits realized with coplanar waveguide resonators terminated by SQUIDS and SQUID arrays, as usually designed for operation as microwave parametric amplifiers (see *e.g.* [35] for a review). Conceptually similar systems using pumped nonlinear crystals have been realized with optical photons [36, 37].

We are therefore interested in the following two scenarios.

- i) The reference dimensionless frequency Ω is of the order of unity or smaller and $\delta\Omega/\Omega \ll 1$. The three symplectic eigenvalues are $\nu_{\pm} = \coth(\frac{\Omega}{2})(1 \mp \frac{\Omega}{\sinh(\Omega)} \frac{\delta\Omega}{\Omega})$ and $\nu = \coth(\frac{\Omega}{2})$ to first order in $\mathcal{O}(\frac{\delta\Omega}{\Omega})$.
- ii) The largest frequency $\Omega - \delta\Omega \gg 1$, or the thermal energy available is extremely low compared to the energy-cost of each excitation. This implies that we can safely set $\nu_m = 1$ for each mode.

We proceed with the analysis of each scenario.

A. Modes with closely separated frequencies

Let us assume that Ω is of the order of unity or smaller and $\delta\Omega/\Omega \ll 1$. This occurs in superconducting circuits when the temperatures are (much) higher than $T = 10\text{mK}$. This is the regime where the initial mixedness due to temperature can be important and the frequencies are “close enough”.

Let us start by noting that, independently of the temperature, one has $\delta\omega/\omega = 2 \times 10^{-3} \ll 1$ in superconducting circuits. One can see that,

$$\nu_{\pm} = \coth(\frac{\Omega}{2})(1 \mp \frac{\Omega}{\sinh(\Omega)} \frac{\delta\Omega}{\Omega}), \quad (36)$$

where the factor $\frac{\Omega}{\sinh(\Omega)}$, in this regime, is a number close to unity.

In this case, we see that the symplectic eigenvalues ν_{\pm} and ν coincide to very good approximation and we ignore contributions of the order $\mathcal{O}(\frac{\delta\Omega}{\Omega})$. We can therefore obtain the elements of the covariance matrix $\boldsymbol{\sigma}$ of the final state (20) which, to lowest order, reduce to

$$\begin{aligned} \alpha &= \nu \cosh(2r_{ab}), \\ \beta &= \nu [\cosh(2r_{ab}) \cosh^2(r_{bc}) + \sinh^2(r_{bc})], \\ \gamma &= \nu [\cosh(2r_{ab}) \sinh^2(r_{bc}) + \cosh^2(r_{bc})], \\ \delta &= \nu \sinh(2r_{ab}) \sinh(r_{bc}), \\ \epsilon &= \nu \sinh(2r_{ab}) \cosh(r_{bc}), \\ \zeta &= \nu \cosh^2(r_{ab}) \sinh(2r_{bc}). \end{aligned} \quad (37)$$

These simplified terms allow us to obtain better analytical understanding of our system, since they dramatically reduce the algebra involved when computing relevant figures of merit.

In particular, we can focus on the smallest symplectic eigenvalues of the reduced states, since they contain all the necessary information to determine quantum correlations. It is easy to check that the smallest symplectic eigenvalues $\tilde{\nu}_{-}^{(ab)}$, $\tilde{\nu}_{-}^{(bc)}$ and $\tilde{\nu}_{-}^{(ac)}$ of the reduced states of modes (ab), (bc) and (ac) respectively are

$$\begin{aligned}
\tilde{\nu}_-^{(ab)} &= \nu \left[1 + 2 \operatorname{sh}_{ab}^2 + \operatorname{sh}_{bc}^2 + \operatorname{sh}_{ab}^2 \operatorname{sh}_{bc}^2 - \sqrt{4 \operatorname{sh}_{ab}^2 + 4 \operatorname{sh}_{ab}^4 + \operatorname{sh}_{bc}^4 + 4 \operatorname{sh}_{ab}^2 \operatorname{sh}_{bc}^2 + 2 \operatorname{sh}_{ab}^2 \operatorname{sh}_{bc}^4 + 4 \operatorname{sh}_{ab}^4 \operatorname{sh}_{bc}^2 + \operatorname{sh}_{ab}^4 \operatorname{sh}_{bc}^4} \right], \\
\tilde{\nu}_-^{(bc)} &= \nu \left[1 + \operatorname{sh}_{ab}^2 + 2 \operatorname{sh}_{bc}^2 + 2 \operatorname{sh}_{ab}^2 \operatorname{sh}_{bc}^2 - \sqrt{\operatorname{sh}_{ab}^4 + 4(1 + \operatorname{sh}_{ab}^2)^2 \operatorname{sh}_{bc}^2 (1 + \operatorname{sh}_{bc}^2)} \right], \\
\tilde{\nu}_-^{(ac)} &= \nu \left[\sqrt{1 + 2 \operatorname{sh}_{ab}^2 + 2 \operatorname{sh}_{bc}^2 + \operatorname{sh}_{ab}^4 + \operatorname{sh}_{bc}^4 + 2 \operatorname{sh}_{ab}^2 \operatorname{sh}_{bc}^4 + \operatorname{sh}_{ab}^4 \operatorname{sh}_{bc}^4} - |\operatorname{sh}_{ab}^2 - \operatorname{sh}_{bc}^2 - \operatorname{sh}_{ab}^2 \operatorname{sh}_{bc}^2| \right]. \tag{38}
\end{aligned}$$

These smallest symplectic eigenvalues are not always smaller than one, i.e., it is not always guaranteed that there is entanglement between the modes in the reduced subsystem. We see that the conditions $\tilde{\nu}_-^{(nm)} \leq 1$ for the existence of the entanglement in the reduced states (ab),(bc) and (ac) are, respectively,

$$\begin{aligned}
\operatorname{sh}_{ab}^2 &\geq \left(\frac{\nu - 1}{2\nu} \right)^2 + \frac{\nu - 1}{2\nu} [2 \operatorname{sh}_{ab}^2 + \operatorname{sh}_{bc}^2 + \operatorname{sh}_{ab}^2 \operatorname{sh}_{bc}^2], \\
\operatorname{sh}_{bc}^2 &\geq \left(\frac{\nu - 1}{2\nu} \right)^2 + \frac{\nu - 1}{2\nu} [\operatorname{sh}_{ab}^2 + 2 \operatorname{sh}_{bc}^2 + 2 \operatorname{sh}_{ab}^2 \operatorname{sh}_{bc}^2], \tag{39}
\end{aligned}$$

and

$$\begin{aligned}
\frac{1 - \nu^2}{\nu^2} &\geq \frac{2}{\nu} |\operatorname{sh}_{ab}^2 - \operatorname{sh}_{bc}^2 - \operatorname{sh}_{ab}^2 \operatorname{sh}_{bc}^2| \\
&\quad + 2 \operatorname{sh}_{ab}^2 + 2 \operatorname{sh}_{bc}^2 + 2 \operatorname{sh}_{ab}^2 \operatorname{sh}_{bc}^2 + 2 \operatorname{sh}_{ab}^4 \operatorname{sh}_{bc}^2. \tag{40}
\end{aligned}$$

We notice that the two conditions in (39) are not always satisfied, which means that there is need for a finite amount of squeezing before any correlation can be established. This is in agreement with previous work that has analysed the interplay of initial mixedness, due to temperature, and squeezing [38]. The exact value of the squeezings, as a function of the initial mixedness ν , at which entanglement is created can be found by looking at the point of saturation of the inequality in these two conditions.

We finally note that the last condition in (40) is never satisfied, since $\nu \geq 1$ and the right hand side is always positive. This is expected from the form of the final state of modes a and c . This means that there is never entanglement between these two modes.

We can also look at the final state (ac) *after* homodyne detection in this regime. As anticipated before, we will now be able to show that the state (34) is entangled. We start by noting that the two reduced states $\sigma_{out|q}^{(a)}$ and $\sigma_{out|q}^{(b)}$ of modes a and c , and the 2×2 correlation block

$\sigma_{out|q}^{(corr)}$, read

$$\begin{aligned}
\sigma_{out|q}^{(a)} &= \begin{pmatrix} \alpha - \frac{\epsilon^2}{2\beta} & -\frac{\epsilon^2}{2\beta} \\ -\frac{\epsilon^2}{2\beta} & \alpha - \frac{\epsilon^2}{2\beta} \end{pmatrix}, \\
\sigma_{out|q}^{(b)} &= \begin{pmatrix} \gamma - \frac{\zeta^2}{2\beta} & -\frac{\zeta^2}{2\beta} \\ -\frac{\zeta^2}{2\beta} & \gamma - \frac{\zeta^2}{2\beta} \end{pmatrix}, \\
\sigma_{out|q}^{(corr)} &= \begin{pmatrix} \delta - \frac{\epsilon\zeta}{2\beta} & -\frac{\epsilon\zeta}{2\beta} \\ -\frac{\epsilon\zeta}{2\beta} & \delta - \frac{\epsilon\zeta}{2\beta} \end{pmatrix}. \tag{41}
\end{aligned}$$

We then introduce the *local symplectic invariants* a^2, b^2 and $c_+ c_-$, defined as $a^2 := \det(\sigma_{out|q}^{(a)})$, $b^2 := \det(\sigma_{out|q}^{(b)})$ and $c_+ c_- := \det(\sigma_{out|q}^{(corr)})$. We notice that a two-mode entangled state is *symmetric* if, in a decomposition of this form, $a^2 = b^2$, see [13]. In our case we have

$$\begin{aligned}
a^2 = b^2 &= \nu^2 \frac{(1 + 2 \operatorname{sh}_{bc}^2 + 2 \operatorname{sh}_{ab}^2 \operatorname{sh}_{bc}^2)(1 + 2 \operatorname{sh}_{ab}^2)}{1 + 2 \operatorname{sh}_{ab}^2 + 2 \operatorname{sh}_{bc}^2 + 2 \operatorname{sh}_{ab}^2 \operatorname{sh}_{bc}^2} \\
c_+ c_- &= -4\nu^2 \frac{(1 + \operatorname{sh}_{ab}^2) \operatorname{sh}_{ab}^2 \operatorname{sh}_{bc}^2}{1 + 2 \operatorname{sh}_{ab}^2 + 2 \operatorname{sh}_{bc}^2 + 2 \operatorname{sh}_{ab}^2 \operatorname{sh}_{bc}^2}. \tag{42}
\end{aligned}$$

which confirms that we have a symmetric two-mode Gaussian state. It is known that every two mode symmetric Gaussian state is equivalent to a two-mode squeezed state up to local operations [13]. This implies that we can anticipate squeezing between modes a and c , which we proceed to compute.

As done before, we can compute the smallest symplectic eigenvalue $\tilde{\nu}_{-out|q}$ of the partial transpose in order to quantify the squeezing between the two modes. This can be done by employing a known relation between the local symplectic eigenvalues, which has the expression $2(\tilde{\nu}_{-out|q})^2 = \tilde{\Delta} - \sqrt{\tilde{\Delta}^2 - 4 \det(\sigma_{out|q}^{(ac)})}$, where we have introduced $\tilde{\Delta} := a^2 + b^2 - 2 c_+ c_-$ for convenience of presentation. In our case this expression simplifies to

$$(\tilde{\nu}_{-out|q})^2 = a^2 - c_+ c_- - \sqrt{(a^2 - c_+ c_-)^2 - \det(\sigma_{out|q}^{(ac)})}, \tag{43}$$

which allows us immediately find the condition, analogous to (39) and (40), for the existence of the entanglement in this case. We have

$$\frac{(1 + \operatorname{sh}_{ab}^2) \operatorname{sh}_{ab}^2 \operatorname{sh}_{bc}^2}{1 + 2 \operatorname{sh}_{ab}^2 + 2 \operatorname{sh}_{bc}^2 + 2 \operatorname{sh}_{ab}^2 \operatorname{sh}_{bc}^2} \geq \left(\frac{\nu^2 - 1}{4\nu} \right)^2. \tag{44}$$

We can immediately see that, if $r_{ab} = 0$ or $r_{bc} = 0$, then the condition (44) is never satisfied and there is no entanglement in the state (ac) after homodyne detection.

We can provide an explicit expression for the smallest symplectic eigenvalue $\tilde{\nu}_-^{out|q}$ of the partial transpose and we choose to provide it in Appendix D to avoid printing cumbersome expressions in the main text.

B. Low temperatures

We can now investigate the “low enough” temperature regime. We have seen that, both on superconducting circuits and in optical cavities, $\Omega \gg 1$. In particular, $\Omega = 15$ for microwaves and $\Omega = 84.6$ for optical cavities. This implies that, in both scenarios, $\coth(\Omega_m) \sim 1 - 2 \exp[-\Omega_m]$ which, for all purposes, is unity. The discussion in this section applies as long as $\delta\Omega/\Omega \ll 1$ as well.

The consequence of these considerations is that we can safely set $\nu = 1$ in the results of the previous section. This implies that the symplectic eigenvalues will now read, to leading order,

$$\begin{aligned} \tilde{\nu}_-^{(ab)} &= 1 + 2 \operatorname{sh}_{ab}^2 + \operatorname{sh}_{bc}^2 + \operatorname{sh}_{ab}^2 \operatorname{sh}_{bc}^2 - \sqrt{4 \operatorname{sh}_{ab}^2 + 4 \operatorname{sh}_{ab}^4 + \operatorname{sh}_{bc}^4 + 4 \operatorname{sh}_{ab}^2 \operatorname{sh}_{bc}^2 + 2 \operatorname{sh}_{ab}^2 \operatorname{sh}_{bc}^4 + 4 \operatorname{sh}_{ab}^4 \operatorname{sh}_{bc}^2 + \operatorname{sh}_{ab}^4 \operatorname{sh}_{bc}^4}, \\ \tilde{\nu}_-^{(bc)} &= 1 + \operatorname{sh}_{ab}^2 + 2 \operatorname{sh}_{bc}^2 + 2 \operatorname{sh}_{ab}^2 \operatorname{sh}_{bc}^2 - \sqrt{\operatorname{sh}_{ab}^4 + 4(1 + \operatorname{sh}_{ab}^2)^2 \operatorname{sh}_{bc}^2 (1 + \operatorname{sh}_{bc}^2)}, \\ \tilde{\nu}_-^{(ac)} &= \sqrt{1 + 2 \operatorname{sh}_{ab}^2 + 2 \operatorname{sh}_{bc}^2 + \operatorname{sh}_{ab}^4 + \operatorname{sh}_{bc}^4 + 2 \operatorname{sh}_{ab}^2 \operatorname{sh}_{bc}^4 + \operatorname{sh}_{ab}^4 \operatorname{sh}_{bc}^4} - |\operatorname{sh}_{ab}^2 - \operatorname{sh}_{bc}^2 - \operatorname{sh}_{ab}^2 \operatorname{sh}_{bc}^2|, \end{aligned} \quad (45)$$

which also implies that the conditions (39), (40) and (44) for the existence of entanglement reduce to

$$\begin{aligned} \operatorname{sh}_{ab}^2 &\geq 0, \\ 1 &\geq \frac{1}{2} (1 - \operatorname{th}_{ab}^2) \frac{1 - \operatorname{th}_{bc}^2}{1 + \operatorname{th}_{bc}^2}, \\ 0 &\geq \frac{2}{\nu} |\operatorname{sh}_{ab}^2 - \operatorname{sh}_{bc}^2 - \operatorname{sh}_{ab}^2 \operatorname{sh}_{bc}^2| \\ &\quad + 2 \operatorname{sh}_{ab}^2 + 2 \operatorname{sh}_{bc}^2 + 2 \operatorname{sh}_{ab}^2 \operatorname{sh}_{bc}^2 + 2 \operatorname{sh}_{ab}^4 \operatorname{sh}_{bc}^2, \\ \operatorname{sh}_{ab}^2 \operatorname{sh}_{bc}^2 &\geq 0. \end{aligned} \quad (46)$$

The first two and the last conditions in (46) are always satisfied. This can be easily explained by the fact that there is no initial mixedness that competes with the establishment of correlations between the different modes. That these conditions are always satisfied, it can be seen from Figures 2, i.e., from the fact that the curve for this case is always positive, except for the origin. For completeness, we can use (22) to find the average excitation in this low temperature regime. We find

$$\begin{aligned} \langle a^\dagger a \rangle &= \operatorname{sh}_{ab}^2 \\ \langle b^\dagger b \rangle &= \operatorname{sh}_{ab}^2 + \operatorname{sh}_{bc}^2 + \operatorname{sh}_{ab}^2 \operatorname{sh}_{bc}^2 \\ \langle c^\dagger c \rangle &= \operatorname{sh}_{bc}^2 (1 + \operatorname{sh}_{ab}^2). \end{aligned} \quad (47)$$

The third condition in (46) is never satisfied, again, as expected. This implies that in the (ac) state after homodyne there are genuine correlations irrespectively of the amount of initial squeezing. This is surprising, since one can argue that, after the application of the two mode squeezing operators on modes a and b , the reduced state

of a is a thermal state with local temperature T_b determined by

$$T_b = \frac{\hbar \omega}{k_B} \frac{1}{\ln \left(\frac{1 + \operatorname{sh}_{ab}^2 + \operatorname{sh}_{bc}^2 + \operatorname{sh}_{ab}^2 \operatorname{sh}_{bc}^2}{\operatorname{sh}_{ab}^2 + \operatorname{sh}_{bc}^2 + \operatorname{sh}_{ab}^2 \operatorname{sh}_{bc}^2} \right)}, \quad (48)$$

which can be derived by equating $\nu_b = \coth(\frac{\Omega_b}{2}) = 2 \langle b^\dagger b \rangle + 1$, see (47).

This concludes our analysis of the low temperature regime. We emphasize, once more, that this regime is relevant for the experimental applications that are being considered in the present [6].

VI. CONCLUSIONS

We have studied a specific tripartite state of interest for physical implementations in the laboratory, namely a bi-squeezed state. This state can be obtained by applying simultaneous two-mode squeezing between two pairs of modes which share a common third one. We have employed techniques from continuous variables to compute analytically most quantities of interest, such as genuine tri-partite and bipartite entanglement, as well as the purity of all subsystems. We have also analysed the effect of homodyne detection of the common mode, with the aim of acquiring information of the final reduced state of the other two modes. We have found that the modes acquire squeezing-type quantum correlations (nonzero entanglement) after the homodyne detection at the expense of a reduction in coherence.

We have then studied different physically scenarios of relevance for concrete applications, such as low tempera-

tures or modes with very close frequencies. These situations occur in experiments with superconducting circuits aimed at developing the next generation of quantum technologies based on continuous variables.

ACKNOWLEDGMENTS

We thank Marcus Huber, Pertti Hakonen, and Gerardo Adesso for useful comments and discussions. D.E.B. acknowledges hospitality from the University of Vienna and the Hebrew University of Jerusalem, where part of this project was done. Financial support from Fundación General CSIC (Programa ComFuturo) is acknowledged by C.S. G.S.P thanks FQXi, Centre of Quantum Engineering at Aalto University (project QMET), and the Academy of Finland (project 263457 and project 25020 - Centre of Excellence "Low Temperature Quantum Phenomena and Devices) for financial support.

Appendix A: Bi-squeezed tripartite Gaussian states

We start by analysing the subset $\{G_{ab}, G_{bc}, B_{ac}\}$ of all the possible 21 Hermitian operators that are quadratic in the creation and annihilation operators of the modes a, b, c (or, equivalently, in the quadrature operators). Here we have defined

$$\begin{aligned} G_{ab} &:= a^\dagger b^\dagger + a b, \\ G_{bc} &:= b^\dagger c^\dagger + b c, \\ B_{ac} &:= i [a c^\dagger - c a^\dagger]. \end{aligned} \quad (\text{A1})$$

$$R_{ab} G_{ab} + R_{bc} G_{bc} = \dot{\theta}_{ac} B_{ac} + \dot{r}_{ab} e^{i \theta_{ac} B_{ac}} G_{ab} e^{-i \theta_{ac} B_{ac}} + \dot{r}_{bc} e^{i \theta_{ac} B_{ac}} e^{i r_{ab} G_{ab}} G_{bc} e^{-i r_{ab} G_{ab}} e^{-i \theta_{ac} B_{ac}}, \quad (\text{A6})$$

which will provide us the functions $r_{ab}(x), r_{bc}(x)$ and $\theta_{ac}(x)$, as a function of R_{ab}, R_{bc} and x . Notice that the dot stands for derivative with respect to x . Finally, we need to set $x = 1$ in order to find the parameters r_{ab}, r_{bc} and θ_{ac} that we are looking for.

Using the fact that

$$\begin{aligned} e^{i r_{ab} G_{ab}} G_{bc} e^{-i r_{ab} G_{ab}} &= \cosh r_{ab} G_{bc} + \sinh r_{ab} B_{ac}, \\ e^{i r_{bc} G_{bc}} B_{ac} e^{-i r_{bc} G_{bc}} &= \cosh r_{bc} B_{ac} - \sinh r_{bc} G_{ab}, \\ e^{i r_{ab} G_{ab}} B_{ac} e^{-i r_{ab} G_{ab}} &= \cosh r_{ab} B_{ac} + \sinh r_{ab} G_{bc}, \\ e^{i \theta_{ac} B_{ac}} G_{ab} e^{-i \theta_{ac} B_{ac}} &= \cos \theta_{ac} G_{ab} - \sin \theta_{ac} G_{bc}, \\ e^{i \theta_{ac} B_{ac}} G_{bc} e^{-i \theta_{ac} B_{ac}} &= \cos \theta_{ac} G_{bc} + \sin \theta_{ac} G_{ab}, \end{aligned} \quad (\text{A7})$$

It is easy to check that the operators G_{ab}, G_{bc} and B_{ac} form a closed sub-Lie algebra of the full algebra. In fact

$$\begin{aligned} [G_{ab}, G_{bc}] &= -i B_{ac}, \\ [B_{ac}, G_{ab}] &= i G_{bc}, \\ [B_{ac}, G_{bc}] &= -i G_{ab}. \end{aligned} \quad (\text{A2})$$

Squeezing modes a and b at the same time as modes b and c , with parameters R_{ab} and R_{bc} respectively can be done through the unitary operator

$$U = e^{i [R_{ab} G_{ab} + R_{bc} G_{bc}]} \quad (\text{A3})$$

It has been shown, see [22], that the operator (A3) can be written as

$$U = e^{i \theta_{ac} B_{ac}} e^{i r_{ab} G_{ab}} e^{i r_{bc} G_{bc}}, \quad (\text{A4})$$

where the real functions r_{ab}, r_{bc} and θ_{ac} depend on R_{ab} and R_{bc} .

It is possible to find r_{ab}, r_{bc} and θ_{ac} as functions of R_{ab} and R_{bc} . To do this we introduce

$$U(x) := e^{i [R_{ab} G_{ab} + R_{bc} G_{bc}] x}, \quad (\text{A5})$$

where we notice that $U(1)$ just coincides with the operator (A3) we are interested in. We then use the techniques introduced in [22], which prescribe to perform differentiation with respect to x on the left and right side of (A5) and the multiply both sides on the right by $U^\dagger(x)$. We obtain the main differential equation

we obtain the main differential equations

$$\begin{aligned} \dot{r}_{ab} \cos \theta_{ac} + \dot{r}_{bc} \sin \theta_{ac} \cosh r_{ab} &= R_{ab}, \\ -\dot{r}_{ab} \sin \theta_{ac} + \dot{r}_{bc} \cos \theta_{ac} \cosh r_{ab} &= R_{bc}, \\ \dot{\theta}_{ac} + \dot{r}_{bc} \sinh r_{ab} &= 0. \end{aligned} \quad (\text{A8})$$

Let us introduce

$$\begin{aligned} \rho &:= \sqrt{R_{ab}^2 + R_{bc}^2}, \\ \tan \phi &:= \frac{R_{bc}}{R_{ab}}. \end{aligned} \quad (\text{A9})$$

We can now rewrite the main differential equations (A8) as

$$\begin{aligned} \dot{r}_{ab} &= \rho \cos(\phi + \theta_{ac}), \\ \dot{r}_{bc} \cosh r_{ab} &= \rho \sin(\phi + \theta_{ac}), \\ \dot{\theta}_{ac} + \dot{r}_{bc} \sinh r_{ab} &= 0. \end{aligned} \quad (\text{A10})$$

Combining the equations in (A10) we obtain

$$\dot{\theta}_{ac} \cot(\phi + \theta_{ac}) = -\dot{r}_{ab} \tanh r_{ab}, \quad (\text{A11})$$

which can be written as

$$\frac{d}{dx} \ln \sin(\phi + \theta_{ac}) = -\frac{d}{dx} \ln \cosh r_{ab}. \quad (\text{A12})$$

This gives the following important relation

$$\sin(\phi + \theta_{ac}) = \frac{\sin \phi}{\cosh r_{ab}}, \quad (\text{A13})$$

where we have used the initial conditions $r_{ab}(x = 0) = 0$ and $\theta_{ac}(x = 0) = 0$. Notice also that ϕ is defined in terms of R_{ab} and R_{bc} and does not depend on x .

Using this equation we obtain the first important relation

$$\sinh r_{ab} = \cos \phi \sinh(\rho x), \quad (\text{A14})$$

which immediately allows us to find

$$\sin(\phi + \theta_{ac}) = \frac{\sin \phi}{\sqrt{1 + \cos^2 \phi \sinh^2(\rho x)}}. \quad (\text{A15})$$

Finally, combining all equations we obtain

$$\dot{r}_{bc} = \rho \frac{\sin \phi}{1 + \cos^2 \phi \sinh^2(\rho x)}, \quad (\text{A16})$$

which leads to

$$r_{bc} = \frac{1}{2} \ln \left[\frac{1 + \sin \phi \tanh(\rho x)}{1 - \sin \phi \tanh(\rho x)} \right]. \quad (\text{A17})$$

We are finally in the position to obtain the desired relations between r_{ab} , r_{bc} and θ_{ac} . All we need to do is set $x = 1$ in the main relations (A14), (A15) and (A17), and invert them. We find

$$\begin{aligned} r_{ab} &= \ln \left(\cos \phi \sinh \rho + \sqrt{1 + \cos^2 \phi \sinh^2 \rho} \right), \\ r_{bc} &= \frac{1}{2} \ln \left(\frac{1 + \sin \phi \tanh \rho}{1 - \sin \phi \tanh \rho} \right), \\ \theta_{ac} &= \arctan \left(\frac{\tan \phi}{\cosh \rho} \right) - \phi. \end{aligned} \quad (\text{A18})$$

Notice the following. Let $R_{bc} = 0$, which implies $\rho = R_{ab}$ and $\phi = 0$. Then $r_{ab} = R_{ab}$, $r_{bc} = 0$ and $\theta_{ac} = 0$ as expected. Now let $R_{ab} = 0$, which implies $\rho = R_{bc}$ and $\phi = \pi/2$. Then $r_{ab} = 0$, $r_{bc} = R_{bc}$ and $\theta_{ac} = 0$, again, as expected.

Appendix B: Elements of the covariance matrix of the final state

Here we reproduce the entries of the final state (20), given that the initial state is thermal, with Williamson form $\sigma_{th} = \text{diag}(\nu_a, \nu_b, \nu_c, \nu_a, \nu_b, \nu_c)$. The algebra necessary to obtain them is straightforward, although cumbersome and not-illuminating. For this reason we present the final results only. We have

$$\begin{aligned} \alpha &:= (\nu_a + (\nu_c - \nu_a) \sin^2 \theta_{ac}) \cosh^2 r_{ab} + \nu_b \sinh^2 r_{ab}, \\ \beta &:= \nu_b \cosh^2 r_{ab} \cosh^2 r_{bc} \\ &\quad + (\nu_a + (\nu_c - \nu_a) \sin^2 \theta_{ac}) \sinh^2 r_{ab} \cosh^2 r_{bc} \\ &\quad - \frac{(\nu_c - \nu_a)}{2} \sin(2 \theta_{ac}) \sinh r_{ab} \sinh(2 r_{bc}) \\ &\quad + (\nu_c - (\nu_c - \nu_a) \sin^2 \theta_{ac}) \sinh^2 r_{bc}, \\ \gamma &:= (\nu_c - (\nu_c - \nu_a) \sin^2 \theta_{ac}) \cosh^2 r_{bc} \\ &\quad - \frac{(\nu_c - \nu_a)}{2} \sin^2 \theta_{ac} \sinh r_{ab} \sinh(2 r_{bc}) \\ &\quad + \nu_b \cosh^2 r_{ab} \sinh^2 r_{bc} \\ &\quad + (\nu_a + (\nu_c - \nu_a) \sin^2 \theta_{ac}) \sinh^2 r_{ab} \sinh^2 r_{bc}, \\ \delta &:= -\frac{1}{2} (\nu_c - \nu_a) \sin(2 \theta_{ac}) \cosh r_{bc} \cosh r_{ab} \\ &\quad + \frac{1}{2} (\nu_b + \nu_a + (\nu_c - \nu_a) \sin^2 \theta_{ac}) \sinh(2 r_{ab}) \sinh r_{bc}, \\ \epsilon &:= \frac{1}{2} \sinh(2 r_{ab}) \cosh r_{bc} (\nu_b + \nu_a + (\nu_c - \nu_a) \sin^2 \theta_{ac}) \\ &\quad - \frac{(\nu_c - \nu_a)}{2} \sin(2 \theta_{ac}) \sinh r_{bc} \cosh r_{ab}, \\ \zeta &:= \frac{1}{4} (-2 (\nu_c - \nu_a) \cosh(2 r_{bc}) \sin(2 \theta_{ac}) \sinh r_{ab} \\ &\quad + (\nu_a + 2 \nu_b + \nu_c) \cosh^2 r_{ab} \sinh(2 r_{bc}) \\ &\quad - (\nu_c - \nu_a) \cos(2 \theta_{ac}) (\sinh^2 r_{ab} - 1) \sinh(2 r_{bc})). \end{aligned} \quad (\text{B1})$$

Appendix C: The smallest symplectic eigenvalue of the partial transpose after homodyne detection

In this section we derive the expression of the covariance matrix of modes a and c after homodyne detection of mode b .

We start by adapting our vectors and covariance matrices to the notation used in [31]. In particular, we need to change the basis of the vector of operators \mathbb{X} , and consequently the covariance matrix, from the one we adopted in this work to

$$\mathbb{X} = (q_a, p_a, q_c, p_c, q_b, p_b)^{\text{Tp}}, \quad (\text{C1})$$

where $q_a = a + a^\dagger$, $p_a = -i(a - a^\dagger)$ are the position and momentum quadratures of mode a and analogous formulas hold for modes b and c . We choose b as the last mode since it is the one we intend to measure. The

linear operator \mathbf{K} which implements this change of basis is given by the (proportional to) unitary matrix

$$\mathbf{K} = \begin{pmatrix} 1 & 0 & 0 & 1 & 0 & 0 \\ -i & 0 & 0 & i & 0 & 0 \\ 0 & 0 & 1 & 0 & 0 & 1 \\ 0 & 0 & -i & 0 & 0 & i \\ 0 & 1 & 0 & 0 & 1 & 0 \\ 0 & -i & 0 & 0 & i & 0 \end{pmatrix}, \quad (\text{C2})$$

and then the three-mode state of interest in the new basis is given by $\sigma' = \mathbf{K} \sigma \mathbf{K}^\dagger$. This has the expression

$$\sigma' = 2 \begin{pmatrix} \alpha & 0 & \delta & 0 & \epsilon & 0 \\ 0 & \alpha & 0 & \delta & 0 & -\epsilon \\ \delta & 0 & \gamma & 0 & \zeta & 0 \\ 0 & \delta & 0 & \gamma & 0 & -\zeta \\ \epsilon & 0 & \zeta & 0 & \beta & 0 \\ 0 & -\epsilon & 0 & -\zeta & 0 & \beta \end{pmatrix}. \quad (\text{C3})$$

Now, we can conveniently divide the state σ' matrix as

$$\sigma' = \begin{pmatrix} \mathbf{A} & \mathbf{C} \\ \mathbf{C}^T & \mathbf{B} \end{pmatrix}, \quad (\text{C4})$$

which will prove convenient when applying the formalism of homodyne measurement. Note that \mathbf{A} and \mathbf{B} would be the reduced *ac* and *b* states respectively, while \mathbf{C} contains all the correlations among the *ac* and *b* subsystems. According to [31], if we perform a perfect homodyne detection of the quadrature q_b or p_b , the resulting two-mode (*ac*) state will be respectively

$$\begin{aligned} \sigma_{out|q}^{(ac)} &= \mathbf{A} - (b_1)^{-1} \mathbf{C} \pi \mathbf{C}^T \\ \sigma_{out|p}^{(ac)} &= \mathbf{A} - (b_2)^{-1} \mathbf{C} \pi' \mathbf{C}^T \end{aligned} \quad (\text{C5})$$

where the matrices \mathbf{A} and \mathbf{C} , and the parameter b_1 and b_2 , can be read out of equation (C4) and we need to take into account that the matrix \mathbf{B} and the projectors π and

π' have the expression

$$\mathbf{B} = \begin{pmatrix} b_1 & b_3 \\ b_3 & b_2 \end{pmatrix}, \quad \pi = \begin{pmatrix} 1 & 0 \\ 0 & 0 \end{pmatrix}, \quad \pi' = \begin{pmatrix} 0 & 0 \\ 0 & 1 \end{pmatrix}. \quad (\text{C6})$$

Here π and π' are the projectors associated to a measurement of the quadratures q_b and p_b of mode *b*. As expected, the reduced *ac* state \mathbf{A} is modified by the projective measurement as long as there are some correlations with mode *b* -which are codified in the matrix \mathbf{C} . Note that for the sake of simplicity we are considering that the measurement is perfect, that is the efficiency is 1.

A lengthy computation indicates that $\sigma_{out|p}^{(ac)}$ and $\sigma_{out|q}^{(ac)}$ differ by minus signs and that the resulting symplectic eigenvalues are exactly the same. Therefore, we will restrict ourselves to the analysis of $\sigma_{out|q}^{(ac)}$.

As a straightforward application of equation (C5), we obtain the matrix $\sigma_{out|q}^{(ac)}$ in the notation of [31]. We find

$$\sigma_{out|q}^{(ac)} = 2 \begin{pmatrix} \alpha - \frac{\epsilon^2}{\beta} & 0 & \delta - \frac{\epsilon\zeta}{\beta} & 0 \\ 0 & \alpha & 0 & \delta \\ \delta - \frac{\epsilon\zeta}{\beta} & 0 & \gamma - \frac{\zeta^2}{\beta} & 0 \\ 0 & \delta & 0 & \gamma \end{pmatrix}, \quad (\text{C7})$$

which can be transformed back to the reduced state after homodyne detection in the original basis. We have

$$\sigma_{out|q}^{(ac)} = \begin{pmatrix} \alpha - \frac{\epsilon^2}{2\beta} & \delta - \frac{\epsilon\zeta}{2\beta} & -\frac{\epsilon^2}{2\beta} & -\frac{\epsilon\zeta}{2\beta} \\ \delta - \frac{\epsilon\zeta}{2\beta} & \gamma - \frac{\zeta^2}{2\beta} & -\frac{\epsilon\zeta}{2\beta} & -\frac{\zeta^2}{2\beta} \\ -\frac{\epsilon^2}{2\beta} & -\frac{\epsilon\zeta}{2\beta} & \alpha - \frac{\epsilon^2}{2\beta} & \delta - \frac{\epsilon\zeta}{2\beta} \\ -\frac{\epsilon\zeta}{2\beta} & -\frac{\zeta^2}{2\beta} & \delta - \frac{\epsilon\zeta}{2\beta} & \gamma - \frac{\zeta^2}{2\beta} \end{pmatrix}. \quad (\text{C8})$$

Appendix D: The smallest symplectic eigenvalue of the partial transpose after homodyne detection

We reproduce the full expression of the smallest symplectic eigenvalue $\tilde{\nu}_{-}^{out|q}$ of the partial transpose of the state of modes *a* and *c* after homodyne detection of the modes *b*, and its counterpart for extremely close frequencies (i.e., $\nu_a = \nu_b = \nu_c \equiv \nu$). We have

$$\begin{aligned} 2(\tilde{\nu}_{-}^{out|q})^2 &= \alpha^2 + \gamma^2 - 2\delta^2 - \frac{(\alpha\epsilon^2 - 2\delta\epsilon\xi + \gamma\xi^2)}{\beta} \\ &\quad - \frac{1}{\beta} \sqrt{-4\beta(\alpha\gamma - \delta^2)(\alpha\beta\gamma - \beta\delta^2 - \gamma\epsilon^2 + 2\delta\epsilon\xi - \alpha\xi^2) + (\alpha^2\beta + \beta(\gamma^2 - 2\delta^2) - \alpha\epsilon^2 + \xi(2\delta\epsilon - \gamma\xi))^2} \\ (\tilde{\nu}_{-}^{out|q})^2 &= \frac{1 + 2\text{sh}_{ab}^2 + 2\text{sh}_{bc}^2 + 10\text{sh}_{ab}^2\text{sh}_{bc}^2 + 8\text{sh}_{ab}^4\text{sh}_{ab}^2}{1 + 2\text{sh}_{ab}^2 + 2\text{sh}_{bc}^2 + 2\text{sh}_{ab}^2\text{sh}_{bc}^2} \\ &\quad - 4\text{sh}_{ab}^2\text{sh}_{bc}^2 \frac{\sqrt{1 + 3\text{sh}_{ab}^2 + 2\text{sh}_{bc}^2 + 8\text{sh}_{ab}^2\text{sh}_{bc}^2 + 2\text{sh}_{ab}^4 + 10\text{sh}_{ab}^4\text{sh}_{bc}^2 + 4\text{sh}_{ab}^6\text{sh}_{bc}^2}}{1 + 2\text{sh}_{ab}^2 + 2\text{sh}_{bc}^2 + 2\text{sh}_{ab}^2\text{sh}_{bc}^2}. \end{aligned} \quad (\text{D1})$$

[1] J. Gea-Banacloche, M. O. Scully, and M. S. Zubairy, *Physica Scripta* **1988**, 81 (1988).

[2] G. Paraoanu (Springer, Switzerland, 2015) Chap. 12, pp. 181–197.

[3] G. T. Moore, *J. Math. Phys* **11**, 269 (1970).

[4] N. D. Birrell and P. C. W. Davies, *Quantum Field in Curved Space* (Cambridge University Press, 1984).

[5] C. M. Wilson, G. Johansson, A. Pourkabirian, M. Simoen, J. R. Johansson, T. Duty, F. Nori, and P. Delsing, *Nature* **479**, 376 (2011).

[6] P. Lähteenmäki, G. S. Paraoanu, J. Hassel, and P. J. Hakonen, *Proc. Natl. Acad. Sci.* **110**, 4234 (2013).

[7] J. R. Johansson, G. Johansson, C. M. Wilson, P. Delsing, and F. Nori, *Phys. Rev. A* **87**, 043804 (2013).

[8] C. Sabín, I. Fuentes, and G. Johansson, *Phys. Rev. A* **92**, 012314 (2015).

[9] C. Sabín and G. Adesso, *Phys. Rev. A* **92**, 042107 (2015).

[10] D. E. Bruschi, C. Sabín, P. Kok, G. Johansson, and P. Delsing, *Sci. Rep.* **6**, 18349 (2016).

[11] S. Felicetti, M. Sanz, L. Lamata, G. Romero, G. Johansson, P. Delsing, and E. Solano, *Phys. Rev. Lett.* **113**, 093602 (2014).

[12] P. Lähteenmäki, G. S. Paraoanu, J. Hassel, and P. J. Hakonen, “Coherence from vacuum fluctuations,” (2015), arXiv:1512.05561 [quant-ph].

[13] G. Adesso, S. Ragy, and A. R. Lee, *Open Systems & Information Dynamics* **21**, 1440001 (2014).

[14] J. Williamson, *Amer. J. Math.* **58**, 141 (1936).

[15] J. Williamson, *Amer. J. Math.* **58**, 747 (1936).

[16] V. I. Arnold, *Mathematical Methods of Classical Mechanics* (Springer-Verlag, 1978).

[17] S. Lloyd and S. L. Braunstein, *Phys. Rev. Lett.* **82**, 1784 (1999).

[18] T. D. Ladd, F. Jelezko, R. Laflamme, Y. Nakamura, C. Monroe, and J. L. O’Brien, *Nature* **464**, 45 (2010).

[19] N. Gisin, G. Ribordy, W. Tittel, and H. Zbinden, *Rev. Mod. Phys.* **74**, 145 (2002).

[20] D. F. Walls and G. J. Milburn, *Quantum Optics* (Springer-Verlag, 2008).

[21] J. R. Johansson, G. Johansson, C. M. Wilson, and F. Nori, *Phys. Rev. A* **82**, 052509 (2010).

[22] D. E. Bruschi, A. R. Lee, and I. Fuentes, *Journal of Physics A: Mathematical and Theoretical* **46**, 165303 (2013).

[23] C. Moore and D. E. Bruschi, “Tuneable interacting bosons for relativistic and quantum information processing,” (2016), arXiv:1601.01919 [quant-ph].

[24] E. G. Brown, E. Martín-Martínez, N. C. Menicucci, and R. B. Mann, *Phys. Rev. D* **87**, 084062 (2013).

[25] O. Penrose and L. Onsager, *Phys. Rev.* **104**, 576 (1956).

[26] P. N. re, in *Bose-Einstein Condensation*, edited by A. G. D. W. Snoke and S. Stringari (Cambridge University Press, 1995).

[27] Y. Castin and J. Dalibard, *Phys. Rev. A* **55**, 4330 (1997).

[28] G. S. Paraoanu, *Journal of Low Temperature Physics* **153**, 285 (2008).

[29] E. J. Mueller, T.-L. Ho, M. Ueda, and G. Baym, *Phys. Rev. A* **74**, 033612 (2006).

[30] G. S. Paraoanu, *Phys. Rev. A* **77**, 041605 (2008).

[31] G. Spedalieri, C. Ottaviani, and S. Pirandola, *Open Systems and Information Dynamics* **20**, 1350011 (2013).

[32] J. Li, K. Chalapat, and G. S. Paraoanu, *Phys. Rev. B* **78**, 064503 (2008).

[33] J. Li, K. Chalapat, and G. S. Paraoanu, *Journal of Physics: Conference Series* **150**, 022051 (2009).

[34] M. B. Plenio, S. F. Huelga, A. Beige, and P. L. Knight, *Phys. Rev. A* **59**, 2468 (1999).

[35] P. Lähteenmäki, V. Vesterinen, J. Hassel, G. S. Paraoanu, H. Seppä, and P. Hakonen, *Journal of Low Temperature Physics* **175**, 868 (2014).

[36] N. C. Menicucci, S. T. Flammia, and O. Pfister, *Phys. Rev. Lett.* **101**, 130501 (2008).

[37] M. Chen, N. C. Menicucci, and O. Pfister, *Phys. Rev. Lett.* **112**, 120505 (2014).

[38] D. E. Bruschi, N. Friis, I. Fuentes, and S. Weinfurtner, *New Journal of Physics* **15**, 113016 (2013).